First Angle-Resolved Photoelectron Measurements following Inner-Shell Resonant Excitation in a Singly Charged Ion

S. Al Moussalami, J. M. Bizau, B. Rouvellou,* D. Cubaynes, L. Journel, and F. J. Wuilleumier
Laboratoire de Spectroscopie Atomique et Ionique and Laboratoire pour l'Utilisation du Rayonnement Electromagnétique, Bâtiment 350, Université Paris-Sud, 91405 Orsay Cedex, France

J. Obert and J. C. Putaux
Institut de Physique Nucléaire, Bâtiment 100, Université Paris-Sud, 91405 Orsay Cedex, France

T. J. Morgan
Wesleyan University, Middletown, Connecticut 06457

M. Richter
Technische Universität Berlin, D-10623 Berlin, Germany
(Received 12 January 1996)

We have measured the angular distribution of electrons emitted in the autoionization of the giant resonance $3p^6 4s\,^2S \rightarrow [(3p^5 3d\,^1P)4s]^2P$ in Ca^+ ions over the profile of the resonance. The absolute value of the asymmetry parameter we have determined at the top of the resonance is $\beta = 1.89 \pm 0.13$, suggesting that LS coupling remains a good approximation for the description of this ionic resonance. [S0031-9007(96)00400-0]

PACS numbers: 32.80.Hd, 32.80.Fb

In this paper, we present the results of the first determination of the angular distribution of photoelectrons ejected after resonant excitation of an inner-shell electron in an atomic ion. More specifically, the $3p \rightarrow 3d$ giant resonance in Ca^+ was photoexcited, according to $3p^6 4s\,^2S \rightarrow [(3p^5 3d\,^1P)4s]^2P$, and the electrons emitted in the autoionization of the excited ions $[3p^5 3d 4s\,^2P \rightarrow 3p^6 \varepsilon p\,^2P]$ were detected as a function of electron kinetic energy and direction of emission.

Resonant photoionization plays an important role in studies of multiply charged ion plasmas: Photoexictation of an electron to an empty ionic orbital is related often with a strong enhancement of the photoionization cross sections. For inner-shell excited light ions, autoionization is the most likely decay process to occur. Photoelectron spectroscopy is then the best tool to study the dynamics of the these processes. It gives unique information on the decay paths of the excited ion, as well as on the angular distribution on the electrons emitted during the autoionization.

Several theoretical models have been developed to calculate the parameters of direct and resonant photoionization in a large number of ions [1]. These results suffer a lack of experimental data to test their validity. Most of the experiments carried out up to now have used the dual laser-produced plasma (DLPP) technique for photoabsorption measurements [2,3], bringing information on relative variations of the total cross section and resonance energies. Some of them have merged beams of monochromatized synchrotron radiation (SR) with a singly charged ion beam to measure, by ion spectrometry [4–6], the total yield of the resulting doubly charged ions. Absolute photoionization cross sections of a few singly charged ions were measured, mostly over the energy range corresponding to resonant excitations of inner electrons. More recently, we have demonstrated the feasibility of performing photoelectron spectrometry on ionic species in a beam-beam experiment [7,8]. The advantages of beam-beam experiments are manifold. The ions can be produced in a well defined state; more sophisticated detection techniques, such as photoion or photoelectron spectrometries, can be used, and the photoionization cross sections can be determined on an absolute scale, provided the overlap between the two beams is carefully measured.

The study of giant resonances in atoms has attracted considerable interest during the past two decades [9]. In the case of $np \rightarrow nd$ transions in the heaviest alkaline-earth atoms or ions, these resonances result from the orbital collapse during the photoexcitation of the *np* low-lying inner-shell electron to an *nd* empty subshell. The large overlap between the wave functions describing the inner *np* and the collapsed *nd* atomic subshells is responsible for the very high oscillator strength of these resonances (2.3 in Ca^+). The photon energy dependence of the angular distribution of photoelectrons over the profile of a resonance can exhibit very strong oscillations, resulting from possible interferences between outgoing waves in continuum channels with different momenta [10]. Such oscillations were not observed in the case of the $3p \rightarrow 3d$ giant resonance in neutral Ca for the electrons leaving the Ca^+ ions in the $3p^6 4s$ configuration, according to $3p^4 4s^2\,^1S \rightarrow 3p^5 3d 4s^2\,^1P \rightarrow 3p^6 4s \varepsilon p\,^1P$ [11]. A constant value $\beta = 2$ was determined for the asymmetry parameter over the profile of the resonance,

 0031-9007/96/76(24)/4496(4)$10.00

indicating that *LS* coupling is still a good approximation. However, some departure from the *LS* coupling has been observed in the $4d \rightarrow 4p$ giant resonance of strontium [12], and, recently, in photoemission measurements of atomic chlorine [13]. In the case of Ca^+, the spin-orbit interaction, being proportional to $1/r^3$, must be stronger than in the case of $3p \rightarrow 3d$ giant resonance of Ca. Thus, it is important to explore whether some deviations from *LS* coupling occurs in Ca^+ ions.

The photoexcitation of the $3p \rightarrow 3d$ giant resonance in Ca^+ ions was previously studied both theoretically and experimentally. The excitation energy E_r of the resonance was measured ($E_r = 33.19$ eV) in a photoabsorption experiment [14], and the absolute value of its oscillator strength *f* was determined in a photoion beam-beam measurement [6]. In a previous experiment, we have detected the electrons emitted in the autoionization of the resonance, using angle-integrated photoelectron spectrometry [7,8]. Finally, the coincidence signal between the photoelectrons and the photoions was measured recently over the same energy range [15]. On the theoretical side, the multiconfiguration Hartree-Fock (MCHF) approximation was used to calculate the energy and oscillator strength of the resonance for the $3p^6 4s\,^2S$ ionic state [16] and the $3p^6 3d\,^2D$ metastable state [17]. The photoionization cross section was also calculated in this energy region using the *R*-matrix [18] and random phase (RPAE) [19] approximations. There is no calculation available at this time on the angular distribution on the photoelectron in the resonance.

As in our previous experiments [7,8], we focused a Ca^+ ion beam in the source volume of an electron energy analyzer (CMA) together with a modulated monochromatic photon beam emitted by the SuperACO storage ring in Orsay. After interaction, the photoelectrons were energy analyzed in the CMA, and the current of doubly charged ions produced by photoionization and selected by a second magnet was measured in a Faraday cup. A new high-transmission CMA [20] and new vacuum chambers allowing the detection of the electrons under ultrahigh vacuum conditions (10^{-9} Torr presently) were built, reducing significantly the background of electrons produced by collisional ionization between the ion beam and the residual gas. The electrons emitted around the angle of $\theta_m = 54°44'$, with respect to the direction of ions, in the interaction between the two counterpropagating beams were detected, after energy analysis, by eight identical electron multipliers placed symmetrically in the focal plane of the CMA.

The angle-resolved photoionization cross section can be expressed in the dipole approximation as [21]

$$\frac{d\sigma}{d\Omega} = \frac{\sigma}{4\pi}\left\{1 - \frac{\beta}{2}\left[P_2(\cos\theta) - \frac{3}{2}\right] \times P\sin^2\theta\cos 2(\varphi + \varphi_0)\right\}, \quad (1)$$

where θ and φ are the polar and azimuthal angles describing the direction of emission of the electrons relative to the axis of the CMA and to the main axis of polarization of SR, respectively; P_2 is the second order Legendre polynomial; β is the asymmetry parameter; *P* is the SR linear polarization degree; and φ_0 is the rotation angle of the main axis of the polarization ellipse after the refocusing mirror. In the geometry described above, the angular distribution of the outgoing electrons is obtained by integrating (1) over the sold angle $d\Omega$ seen by each detector. The angular acceptance of one detector is $\Delta\varphi = 9°$. Because of the velocity of the ions (3×10^5 m/sec), the angular acceptance $\Delta\theta$ of the CMA is different in the reference frame of the laboratory and in the reference frame of the ions [22]. Taking into account the effective length of the source volume of the CMA, the angular distribution of the electrons in the laboratory frame can be expressed after integration as

$$\sigma_i \approx C_i\sigma\{1 + 0.495\beta P\cos 2(\varphi_i + \varphi_0)\}, \quad (2)$$

and in the ion frame as

$$\sigma_i \approx C_i\sigma\{1 + 0.567\beta P\cos 2(\varphi_i + \varphi_0)\}, \quad (3)$$

where φ_i is the azimuthal angle for each detector *i*, and C_i is the relative efficiency of the detector *i*. The coefficients C_i have been systematically determined by measuring the angular distribution of the electrons emitted in 2*p*-subshell photoionization of Ne atoms ($\beta = 0.54 \pm 0.02$ at 33.2 eV photon energy [23]). We have checked that the effect of the spiralization of the electrons emitted outside the axis of the CMA is negligible in our geometry ($\Delta\varphi < 2°$). In Eqs. (1) to (3) σ, β, *P*, and φ_0 are functions of the photon energy. *P* and φ_0 have been determined from Eq. (2) by measuring the angular distribution of the photoelectrons emitted in photoionization of He atoms ($\beta = 2$). We found $P = 0.85 \pm 0.03$, and $\varphi_0 = 3.6° \pm 0.8°$ at 33.2 eV photon energy.

Eight photoelectron spectra of Ca^+ ions are recorded simultaneously over the energy range of the giant resonance, each one corresponding to one angle φ_i. Figure 1 shows an example of spectra obtained at 33.2 eV, after correction for the efficiency of each channeltron *i*. We observed here the electron lines produced in the resonance process,

$$\begin{aligned} &Ca^+ 3p^6 4s\,^2S_{1/2} + h\nu(33.2\text{ eV}) \\ &\quad\rightarrow Ca^{+*}[(3p^5 3d)^1P]4s\,^2P_{1/2(3/2)} \\ &\quad\rightarrow Ca^{2+} 3p^6\,^1S_0 + \varepsilon p_{1/2(3/2)}(21.3\text{ eV}), \end{aligned} \quad (4)$$

taking the assignment proposed by Miecznik *et al.* [18]. The difference between expected (21.3 eV) and measured kinetic energy of the electrons (see Fig. 2) results from three different shifts: an accelerating Doppler shift (+2.6 eV), due to the velocity of the ions, and two decelerating shifts, produced by the positive charge of the ion beam (−3 eV) and the contact potentials on the surfaces of the CMA (≈−0.9 eV), respectively. The shift

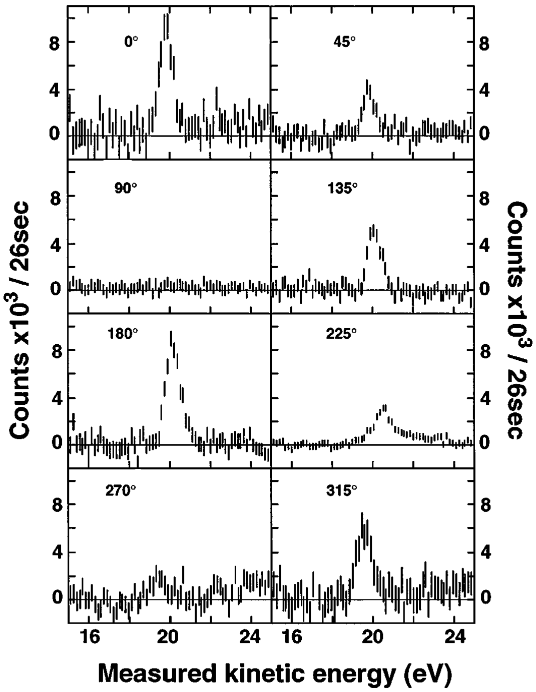

FIG. 1. Photoelectron spectra emitted in the photoionization of Ca^+ ions by 33.2 eV photons, measured simultaneously at eight different azimuthal angles.

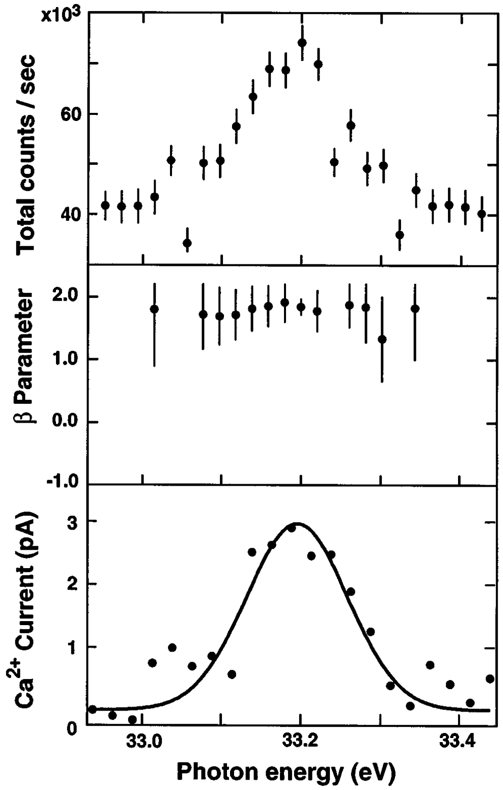

FIG. 2. Upper panel: variation, over the energy range of the resonance, of the sum of the integrated counts of the electron lines recorded simultaneously at the eight angles. Middle panel: variation over the same energy range of the β asymmetry parameter determined at individual photon energies from the spectra recorded at the eight angles. Bottom panel: variation of the yield of Ca^{2+} ions produced in the photoionization of the Ca^+ ion beam; dots show the measured Ca^{2+} current, and the solid line is a Gaussian profile centered at the energy of the resonance (see text).

in the energy position of the lines at some angles φ_i is due to local variation of this contact potential and to slightly different position of some of the detectors.

In order to deduce the asymmetry parameter β from such spectra, we evaluated the integrated area under the electron lines, and fitted the data by formula (3), using β as a free parameter. Varying the photon energy over the profile of the resonance, we obtained the excitation function of the resonance. In the upper panel of Fig. 2 we show the sum of the eight integrated counts. The dispersion of the data at some photon energies is due to fluctuations in the ion beam current. Since the direct 4*s*-photoionization cross section is very weak outside of the resonance, the high electron counting rate we observed on the tails of the resonance in the upper panel is mostly due to some noise produced by stray light caused by defects in the refocusing mirror. From the eight spectra, we determined the variation of the β parameter as shown in the middle panel. The vertical error bars include the contributions of the statistical errors on the integrated counts and substracted background, as well as the uncertainty on the determination of the coefficients C_i. Finally, the excitation function of the resonance obtained from the Ca^{2+} yield is shown in the lower panel of Fig. 2. The absolute uncertainty on these measurements is mainly due to the accuracy of the electrometer, and is of the order of 2 pA.

Both resonance profiles, measured separately from the electron spectra and ion yield, are in good qualitative agreement with each other, as well as with previous photoion measurements [6]. They exhibit a quasi Gaussian shape with a FWHM of about 0.15 eV, resulting from a convolution of our spectral bandpass (0.14 eV) with the natural width of the line (calculated to be between 0.05 eV [18] and 0.06 eV [19]).

Kabachnik and Sazhina [10] have proposed general expressions for the angular distribution of photoelectrons in the region of autoionizing states. As expected, if only one autoionization decay channel is open, the parameter β is independent of the photon energy, i.e., the presence of a resonance does not affect the photoelectron angular distribution. If *LS* coupling is assumed, the two outgoing waves $\varepsilon p_{1/2}$ and $\varepsilon p_{3/2}$ are not separable, and then one should expect a constant value $\beta = 2$. Nevertheless, a strong coupling exists between the giant resonance and double excitation transitions, as confirmed by MCHF calculation [24]. Another indication of the importance of double excitations was given by Ivanov and West

[19] who calculated an oscillator strength $f = 3$ for the giant resonance, while the experimental value is $f = 2.3$. Since their RPAE calculation did not take into account contribution of double excitations, this discrepancy can be attributed to a redistribution of the oscillator strength of the giant resonance into two-electron transition channels.

The values of the asymmetry parameter we have determined over the profile of the resonance are systematically lower than 2. Our most accurate determination is $\beta = 1.89 \pm 0.13$ at the top of the resonance. This value was obtained from six independent measurements. Within the error bar, it is consistent with a constant value $\beta = 2$ expected for an εp wave in the *LS* coupling scheme. This behavior suggests that, in similar fashion to neutral Ca and despite the complexity of the ionic resonance, *LS* coupling remains a good approximation for the description of the giant resonance in the Ca^+ ion. With experimental data on the angular distribution now available for Ca^+, we await new theoretical calculations to further illuminate the physics of giant ion resonances.

The support of the Centre d'Etudes Nucléaires de Limeil-Valenton (CEA-DAM) and EU Human Capital and Mobility Program under Contract No. 93-0361 is gratefully acknowledged.

*Present address: Laboratoire des Collisions Electroniques et Atomiques, 6 Av. Le Gorgeu, BP 809, 29285 Brest Cedex, France.

[1] M. J. Seaton, J. Phys. B **20**, 6363 (1987).
[2] P. K. Carroll, E. T. Kennedy, and G. O'Sullivan, Appl. Opt. **19**, 1454 (1980).
[3] E. Jannitti, P. Nicolosi, and G. Tondello, Opt. Commun. **50**, 225 (1984).
[4] I. C. Lyon, B. Peart, J. West, and K. Dolder, J. Phys. B **19**, 4137 (1986).
[5] I. C. Lyon, P. Peart, K. Dolder, and J. B. West, J. Phys. B **20**, 1471 (1987).
[6] B. Peart, I. C. Lyon, and K. Dolder, J. Phys. B **20**, 5403 (1987).
[7] J. M. Bizau, D. Cubaynes, M. Richter, F. J. Wuilleumier, J. Obert, J. C. Putaux, T. J. Morgan, E. Källne, S. Sorensen, and A. Damany, Phys. Rev. Lett. **67**, 576 (1991).
[8] F. J. Wuilleumier, J. M. Bizau, B. Rouvellou, D. Cubaynes, and L. Journel, Nucl. Instrum. Methods Phys. Res., Sect. B **87**, 190 (1994).
[9] *Giant Resonances in Atoms, Molecules, and Solids*, edited by J. P. Connerade, J. M. Esteva, and R. C. Karnatak, NATO ASI, Ser. B, Vol. 151 (Plenum, New York, 1987).
[10] N. M. Kabachnik and I. P. Sazhina, J. Phys. B **9**, 1681 (1976).
[11] K. Ueda, J. B. West, K. J. Ross, H. Hamdy, H. J. Beyer, and H. Kleinpoppen, Phys. Rev. A **48**, R863 (1993).
[12] K. Ueda, J. B. West, K. J. Ross, H. J. Beyer, H. Hamdy, and H. Kleinpoppen, J. Phys. B **26**, L347 (1993).
[13] M. O. Krause *et al.*, in Proceedings of the XIth Conference on Ultraviolet Radiation Physics, Tokyo, August, 1995 [J. Electron. Spectrosc. Relat. Phenom. (to be published)].
[14] B. F. Sonntag, C. L. Cromer, J. M. Bridges, T. J. McIlrath, and T. B. Lucatorto, in *Short Wavelength Coherent Radiation: Generation and Applications*, edited by D. T. Attwood and J. Bokor, AIP Conf. Proc. Ser. No. 147 (American Institute of Physics, New York, 1986), p. 142.
[15] S. Anger, A. Gottwald, T. Luhmann, D. Rosenthal, M. Richter and J.-M. Bizau, BESSY Jahresbericht report (1994), p. 477.
[16] M. W. D. Mansfield and T. W. Ottley, Proc. R. Soc. London Sect. A **365**, 413 (1979).
[17] J. E. Hansen and P. Quinet, in Proceedings of the XIth Conference on Ultraviolet Radiation Physics, Tokyo, August, 1995 (Ref. [13]).
[18] G. Miecznik, K. A. Berrington, P. G. Burke, and A. Hibbert, J. Phys. B **23**, 3305 (1990).
[19] V. K. Ivanov and J. B. West, J. Phys. B **26**, 2099 (1993).
[20] B. Rouvellou, J. M. Bizau, D. Cubaynes, L. Journel, S. Al Moussalami, and F. J. Wuilleumier, J. Electron. Spectrosc. Related Phenom. **76**, 237 (1995).
[21] V. Schmidt, Phys. Lett. **45A**, 63 (1973).
[22] J. S. Risley, A. K. Edwards, and R. Geballe, Phys. Rev. A **9**, 1115 (1974).
[23] H. Derenbach, R. Malutzki, and V. Schmidt, Nucl. Instrum. Methods Phys. Res. **208**, 845 (1974).
[24] J. E. Hansen, J. Phys. B **8**, 2759 (1975).